Table of Contents (Other Channels)

BACK

Click Channel Type to Access Validation Data:

Table of Contents (Other Channels)

BACK

Please press the “Back” button to return to previous Table of Contents

Click Channel Type to Access Validation Data:

Introduction to TRP Channels

BACK

The founding member of the TRP channel superfamily was identified as an essential component of *Drosophila* phototransduction [1]. A spontaneous mutation in the *trp* gene resulted in a *transient receptor potential* in response to continuous light. Transient receptor potential (TRP) ion channels are comprised of at least 28 distinct genes in mammals. There are six subfamilies by sequence homology: Ankyrin repeat (TRPA), Melastatin (TRPMs), Vanilloid (TRPVs), Canonical (TRPCs), Mucolipins (TRPMLs), Polycystins (TRPPs). TRP channels are generally described as cation permeable channels that function as cellular sensors responding to a broad range of stimuli. They function as cellular sensors integrating multiple stimuli, they are widely expressed, and are active in many physiological processes [2-3]. Most TRP channels promote Na^+ and Ca^{2+} flux into cells, however some some TRP channels primarily span organellar membranes such as endolysosomes [4]. Each TRP channel subunits each are comprised of six transmembrane spanning domains (S1-S6) with four subunits assembling as a tetramer much like voltage-gated K^+ channels.

TRPCs are all thought to be activated downstream of G protein-coupled receptors ($G_{q)}$ and by receptor tyrosine kinases, some TRPs have been shown to be modulated by the phospholipases C (PLC) pathway and production of diacylglycerol (DAG) and inositol-1,4,5-triphosphate (IP_3) [4]. Among the physical stimuli that activate TRP channels, Temperature is known to activate some TRP channels including TRPV1-V4, TRPC5, TRPM3, TRPM5, TRPM8, TRPA1 [5]. Natural products like capsaicin, menthol, and carvacrol, affect TRP channel gating while selective pharmacology is not known for most TRP channels. Capsaicin is the well-known vanilloid in 'hot' peppers and seems to be relatively specific for TRPV1 [8,10]. Blockers including Ruthenium red or 2-APB are not specific. Better tools are emerging with higher potency and more selectivity like the TRPV4 agonist GSK1016790A or its antagonists GSK2193874 and HC-067047, and the TRPA1 antagonist HC-030031 [6-9].

TRP Function and Channelopathies

BACK

TRP channels have been shown to have diverse functions. TRPV1 has been extensively characterized in primary afferent nociceptors and is essential for the perception of noxious stimuli such as heat or capsaicin. It is involved in the development of hyperalgesia following inflammation [6-7]. TRPM8 that is activated by cooling or compounds that evoke a cool sensation such as menthol [12-15]. TRPA1 that is activated by pungent chemicals such as cinnamaldehyde, mustard oil, and allicin, it also contributes to nociception [16-19].

TRP channel gene mutations have been associated with inherited human disease affecting the cardiovascular and nervous systems as well as with renal, skeletal, and epithelial skin diseases [20-21]. Pathogenic mutations in TRP genes have been identified using molecular genetics. These mutations have been shown to cause both loss- and gain-of-function for the channels linked to inherited diseases, but the actual physiological causes of disease are poorly understood. TRP channel signaling has been extensively shown to be tied to changes in intracellular Ca^{2+} levels, these mutations have been hypothesized to affect Ca^{2+}-dependent cellular processes and perhaps even cause toxic Ca^{2+} overload [22].

TRPV4, TRPM6, and PKD2 (TRPP1) have the highest frequency of mutations [20-21]. Different forms of skeletal dysplasia and peripheral neuropathies have been linked to more than 50 pathogenic mutations for TRPV4 [45-46]. TRPV4 mutations have been shown to produce mostly gain-of-function channel properties associated with increased basal Ca^{2+} levels [23,25].

References for TRP Channels

BACK

1) Montell C, Rubin GM. (1989) Molecular characterization of the Drosophila trp locus: a putative integral membrane protein required for phototransduction. *Neuron*, **2** (4): 1313-23. [PMID:2516726]

2) Clapham DE. (2003) TRP channels as cellular sensors. *Nature*, **426** (6966): 517-24. [PMID:14654832]

3) Gees M, Owsianik G, Nilius B, Voets T. (2012) TRP channels. *Compr Physiol*, **2** (1): 563-608. [PMID:23728980]

4) Ramsey IS, Delling M, Clapham DE. (2006) An introduction to TRP channels. *Annu Rev Physiol*, **68**: 619-47. [PMID:16460286]

5) Feng Q. (2014) Temperature sensing by thermal TRP channels: thermodynamic basis and molecular insights. Curr Top Membr, 74: 19-50. [PMID:25366232]

6) Caterina MJ, Leffler A, Malmberg AB, Martin WJ, Trafton J, Petersen-Zeitz KR, Koltzenburg M, Basbaum AI, Julius D. (2000) Impaired nociception and pain sensation in mice lacking the capsaicin receptor. Science, 288 (5464): 306-13. [PMID:10764638]

7) Caterina MJ, Schumacher MA, Tominaga M, Rosen TA, Levine JD, Julius D. (1997) The capsaicin receptor: a heat-activated ion channel in the pain pathway. Nature, 389 (6653): 816-24. [PMID:9349813]

8) Everaerts W, Zhen X, Ghosh D, Vriens J, Gevaert T, Gilbert JP, Hayward NJ, McNamara CR, Xue F, Moran MM *et al.*. (2010) Inhibition of the cation channel TRPV4 improves bladder function in mice and rats with cyclophosphamide-induced cystitis. *Proc Natl Acad Sci USA*, **107** (44): 19084-9. [PMID:20956320]

9) McNamara CR, Mandel-Brehm J, Bautista DM, Siemens J, Deranian KL, Zhao M, Hayward NJ, Chong JA, Julius D, Moran MM *et al.*. (2007) TRPA1 mediates formalin-induced pain. *Proc Natl Acad Sci USA*, **104** (33): 13525-30. [PMID:17686976]

10) Thorneloe KS, Cheung M, Bao W, Alsaid H, Lenhard S, Jian MY, Costell M, Maniscalco-Hauk K, Krawiec JA, Olzinski A *et al.*. (2012) An orally active TRPV4 channel blocker prevents and resolves pulmonary edema induced by heart failure. *Sci Transl Med*, **4** (159): 159ra148. [PMID:23136043]

References for TRP Channels

BACK

11) Thorneloe KS, Sulpizio AC, Lin Z, Figueroa DJ, Clouse AK, McCafferty GP, Chendrimada TP, Lashinger ES, Gordon E, Evans L et al.. (2008) N-((1S)-1-{[4-((2S)-2-{[(2,4-dichlorophenyl)sulfonyl]amino}-3-hydroxypropanoyl)-1-piperazinyl]carbonyl}-3-methylbutyl)-1-benzothiophene-2-carboxamide (GSK1016790A), a novel and potent transient receptor potential vanilloid 4 channel agonist induces urinary bladder contraction and hyperactivity: Part I. J Pharmacol Exp Ther, 326 (2): 432-42. [PMID:18499743]

12) Bautista DM, Siemens J, Glazer JM, Tsuruda PR, Basbaum AI, Stucky CL, Jordt SE, Julius D. (2007) The menthol receptor TRPM8 is the principal detector of environmental cold. Nature, 448 (7150): 204-8. [PMID:17538622]

13) Chuang HH, Neuhausser WM, Julius D. (2004) The super-cooling agent icilin reveals a mechanism of coincidence detection by a temperature-sensitive TRP channel. Neuron, 43 (6): 859-69. [PMID:15363396]

14) McKemy DD, Neuhausser WM, Julius D. (2002) Identification of a cold receptor reveals a general role for TRP channels in thermosensation. Nature, 416 (6876): 52-8. [PMID:11882888]

15) Peier AM, Moqrich A, Hergarden AC, Reeve AJ, Andersson DA, Story GM, Earley TJ, Dragoni I, McIntyre P, Bevan S et al.. (2002) A TRP channel that senses cold stimuli and menthol. Cell, 108 (5): 705-15. [PMID:11893340]

16) Bandell M, Story GM, Hwang SW, Viswanath V, Eid SR, Petrus MJ, Earley TJ, Patapoutian A. (2004) Noxious cold ion channel TRPA1 is activated by pungent compounds and bradykinin. *Neuron*, **41** (6): 849-57. [PMID:15046718]

17) Bautista DM, Jordt SE, Nikai T, Tsuruda PR, Read AJ, Poblete J, Yamoah EN, Basbaum AI, Julius D. (2006) TRPA1 mediates the inflammatory actions of environmental irritants and proalgesic agents. *Cell*, **124** (6): 1269-82. [PMID:16564016]

18) Bautista DM, Movahed P, Hinman A, Axelsson HE, Sterner O, Högestätt ED, Julius D, Jordt SE, Zygmunt PM. (2005) Pungent products from garlic activate the sensory ion channel TRPA1. *Proc Natl Acad Sci USA*, **102** (34): 12248-52. [PMID:16103371]

References for TRP Channels

BACK

19) Jordt SE, Bautista DM, Chuang HH, McKemy DD, Zygmunt PM, Högestätt ED, Meng ID, Julius D. (2004) Mustard oils and cannabinoids excite sensory nerve fibres through the TRP channel ANKTM1. *Nature*, **427** (6971): 260-5. [PMID:14712238]

20) Nilius B, Owsianik G. (2010) Transient receptor potential channelopathies. *Pflugers Arch*, **460** (2): 437-50. [PMID:20127491]

21) Tóth BI, Nilius B. (2015) Transient Receptor Potential Dysfunctions in Hereditary Diseases: TRP Channelopathies and Beyond. *In* TRP Channels as Therapeutic Target *Edited by* Szallasi A (Elsevier Inc) 13-33. DOI: 10.1016/C2013-0-09923-9 [ISBN:9780124200241]

22) Blair NT, Carvacho I, Chaudhuri D, Clapham DE, DeCaen P, Delling M, Doerner JF, Fan L, Grimm CM, Ha K, Jordt SE, Julius D, Kahle KT, Liu B, McKemy D, Nilius B, Oancea E, Owsianik G, Riccio A, Sah R, Stotz SC, Tian J, Tong D, Van den Eynde C, Vriens J, Wu LJ, Xu H, Yue L, Zhang X, Zhu MX. **Transient Receptor Potential channels (TRP) in GtoPdb v.2022.1**. IUPHAR/BPS Guide to Pharmacology CITE. 2022; 2022(1). Available from: https://doi.org/10.2218/gtopdb/F78/2022.1.

23) Nilius B, Voets T. (2013) The puzzle of TRPV4 channelopathies. *EMBO Rep*, **14** (2): 152-63. [PMID:23306656]

24) Nishimura G, Lausch E, Savarirayan R, Shiba M, Spranger J, Zabel B, Ikegawa S, Superti-Furga A, Unger S. (2012) TRPV4-associated skeletal dysplasias. *Am J Med Genet C Semin Med Genet*, **160C** (3): 190-204. [PMID:22791502]

25) Loukin S, Su Z, Kung C. (2011) Increased basal activity is a key determinant in the severity of human skeletal dysplasia caused by TRPV4 mutations. *PLoS One*, **6** (5): e19533. [PMID:21573172]

Introduction to CFTR Channels

BACK

The cystic fibrosis transmembrane conductance regulator (CFTR) is a twelve transmembrane protein, it functions as a cAMP-regulated epithelial membrane Cl^- channel. It is located in the apical membrane and involved in normal salt and fluid transport across epithelial tissues. There have been over 1700 mutations identified in CFTR, the most common is the deletion mutant ΔF508. This results in impaired trafficking of CFTR, reducing its incorporation into the plasma membrane leading to cystic fibrosis [1]. Channels carrying the ΔF508 mutation that do traffic to the plasma membrane also show reduced channel activity. Vertex pharmaceuticals has created combination therapeutics that address both of these issues, both the trafficking problem and it also provides a potentiator function that improves channel function in the apical membrane. Thus, pharmacological restoration of the function of the ΔF508 mutant can be at least partially achieved with these combination therapies.

In addition to acting as an anion channel, CFTR may also regulate other epithelial channels including ENaC (the epithelial Na channel), Ca^{2+}-activated chloride channels, and other conductances [2]. CFTR also regulates TRPV4 in airway epithelia, which provides the Ca^{2+} signal for regulatory volume decrease [3].

CFTR References

BACK

1) Cuthbert AW. (2011) New horizons in the treatment of cystic fibrosis. *Br J Pharmacol*, **163** (1): 173-83. [PMID:21108631]

2) Nilius B, Droogmans G. (2003) Amazing chloride channels: an overview. *Acta Physiol Scand*, **177** (2): 119-47. [PMID:12558550]

3) Arniges M, Vázquez E, Fernández-Fernández JM, Valverde MA. (2004) Swelling-activated Ca2+ entry via TRPV4 channel is defective in cystic fibrosis airway epithelia. *J Biol Chem*, **279** (52): 54062-8. [PMID:15489228]

Introduction to ASIC Channels

eurofins | DiscoverX
The Eurofins Discovery PRODUCTS COMPANY

BACK

Acid-sensing ion channels or ASICs, are members of a Na^+ channel superfamily that includes the epithelial Na^+ channel (ENaC). ASIC subunits contain 2 TM domains and assemble as homo- or hetero-trimers to form proton-gated, voltage-insensitive, Na^+ permeable, channels that are activated by levels of acidosis occurring in both physiological and pathophysiological conditions with ASIC3 also playing a role in mechanosensation [1-5].

One of the most pH-sensitive isoforms ASIC3 [6] has the fastest activation and desensitization kinetics, can still pass a small small sustained current following desensitization. ASIC channels are primarily expressed in central and peripheral neurons including nociceptors (ASIC1-3), there they are responsible for much of the neuronal sensitivity to acidosis. They have also been detected in taste receptor cells, photoreceptors and retinal cells, lung epithelial cells, vascular smooth muscle cells, cochlear hair cells, testis, pituitary, bone adipose and immune cells [7-8].

It has been proposed that protons act like a neurotransmitter, involving postsynaptically located ASICs of the CNS in such basic functions such as fear perception and learning [9-11]. Also in responses to focal ischemia and to axonal degeneration in autoimmune inflammation in a mouse model of multiple sclerosis, as well as seizures and pain [12-19.

The known small molecule inhibitors of ASICs are largely non-selective or partially selective. Venom peptide inhibitors have substantially higher selectivity and potency.

ASIC References

1) Cheng YR, Jiang BY, Chen CC. (2018) Acid-sensing ion channels: dual function proteins for chemo-sensing and mechano-sensing. *J Biomed Sci*, **25** (1): 46. [PMID:29793480]

2) Gründer S, Pusch M. (2015) Biophysical properties of acid-sensing ion channels (ASICs). *Neuropharmacology*, **94**: 9-18. [PMID:25585135]

3) Kellenberger S, Schild L. (2015) International Union of Basic and Clinical Pharmacology. XCI. structure, function, and pharmacology of acid-sensing ion channels and the epithelial Na+ channel. *Pharmacol Rev*, **67** (1): 1-35. [PMID:25287517]

4) Rook ML, Musgaard M, MacLean DM. (2021) Coupling structure with function in acid-sensing ion channels: challenges in pursuit of proton sensors. *J Physiol*, **599** (2): 417-430. [PMID:32306405]

5) Wemmie JA, Taugher RJ, Kreple CJ. (2013) Acid-sensing ion channels in pain and disease. *Nat Rev Neurosci*, **14** (7): 461-71. [PMID:23783197]

6) Waldmann R, Bassilana F, de Weille J, Champigny G, Heurteaux C, Lazdunski M. (1997) Molecular cloning of a non-inactivating proton-gated Na+ channel specific for sensory neurons. *J Biol Chem*, **272** (34): 20975-8. [PMID:9261094]

7) Deval E, Lingueglia E. (2015) Acid-Sensing Ion Channels and nociception in the peripheral and central nervous systems. *Neuropharmacology*, **94**: 49-57. [PMID:25724084]

8) Lin SH, Sun WH, Chen CC. (2015) Genetic exploration of the role of acid-sensing ion channels. *Neuropharmacology*, **94**: 99-118. [PMID:25582292]

9) Du J, Reznikov LR, Price MP, Zha XM, Lu Y, Moninger TO, Wemmie JA, Welsh MJ. (2014) Protons are a neurotransmitter that regulates synaptic plasticity in the lateral amygdala. *Proc Natl Acad Sci USA*, **111** (24): 8961-6. [PMID:24889629]

10) Kreple CJ, Lu Y, Taugher RJ, Schwager-Gutman AL, Du J, Stump M, Wang Y, Ghobbeh A, Fan R, Cosme CV *et al.*. (2014) Acid-sensing ion channels contribute to synaptic transmission and inhibit cocaine-evoked plasticity. *Nat Neurosci*, **17** (8): 1083-91. [PMID:24952644]

BACK

ASIC References

BACK

11) Ziemann AE, Allen JE, Dahdaleh NS, Drebot II, Coryell MW, Wunsch AM, Lynch CM, Faraci FM, Howard 3rd MA, Welsh MJ *et al.*. (2009) The amygdala is a chemosensor that detects carbon dioxide and acidosis to elicit fear behavior. *Cell*, **139** (5): 1012-21. [PMID:19945383]

12) Xiong ZG, Chu XP, Simon RP. (2007) Acid sensing ion channels--novel therapeutic targets for ischemic brain injury. *Front Biosci*, **12**: 1376-86. [PMID:17127388]

13) Friese MA, Craner MJ, Etzensperger R, Vergo S, Wemmie JA, Welsh MJ, Vincent A, Fugger L. (2007) Acid-sensing ion channel-1 contributes to axonal degeneration in autoimmune inflammation of the central nervous system. *Nat Med*, **13** (12): 1483-9. [PMID:17994101]

14) Ziemann AE, Schnizler MK, Albert GW, Severson MA, Howard MA, Welsh MJ, Wemmie JA. (2008) Seizure termination by acidosis depends on ASIC1a. *Nat Neurosci*, **11** (7): 816-22. [PMID:18536711]

15) Bohlen CJ, Chesler AT, Sharif-Naeini R, Medzihradszky KF, Zhou S, King D, Sánchez EE, Burlingame AL, Basbaum AI, Julius D. (2011) A heteromeric Texas coral snake toxin targets acid-sensing ion channels to produce pain. *Nature*, **479** (7373): 410-4. [PMID:22094702]

16) Deval E, Noël J, Gasull X, Delaunay A, Alloui A, Friend V, Eschalier A, Lazdunski M, Lingueglia E. (2011) Acid-sensing ion channels in postoperative pain. *J Neurosci*, **31** (16): 6059-66. [PMID:21508231]

17) Deval E, Noël J, Lay N, Alloui A, Diochot S, Friend V, Jodar M, Lazdunski M, Lingueglia E. (2008) ASIC3, a sensor of acidic and primary inflammatory pain. *EMBO J*, **27** (22): 3047-55. [PMID:18923424]

18) Diochot S, Baron A, Salinas M, Douguet D, Scarzello S, Dabert-Gay AS, Debayle D, Friend V, Alloui A, Lazdunski M *et al.*. (2012) Black mamba venom peptides target acid-sensing ion channels to abolish pain. *Nature*, **490** (7421): 552-5. [PMID:23034652]

19) Wemmie JA, Taugher RJ, Kreple CJ. (2013) Acid-sensing ion channels in pain and disease. *Nat Rev Neurosci*, **14** (7): 461-71. [PMID:23783197]

TRPA1 (CYL3066)

BACK

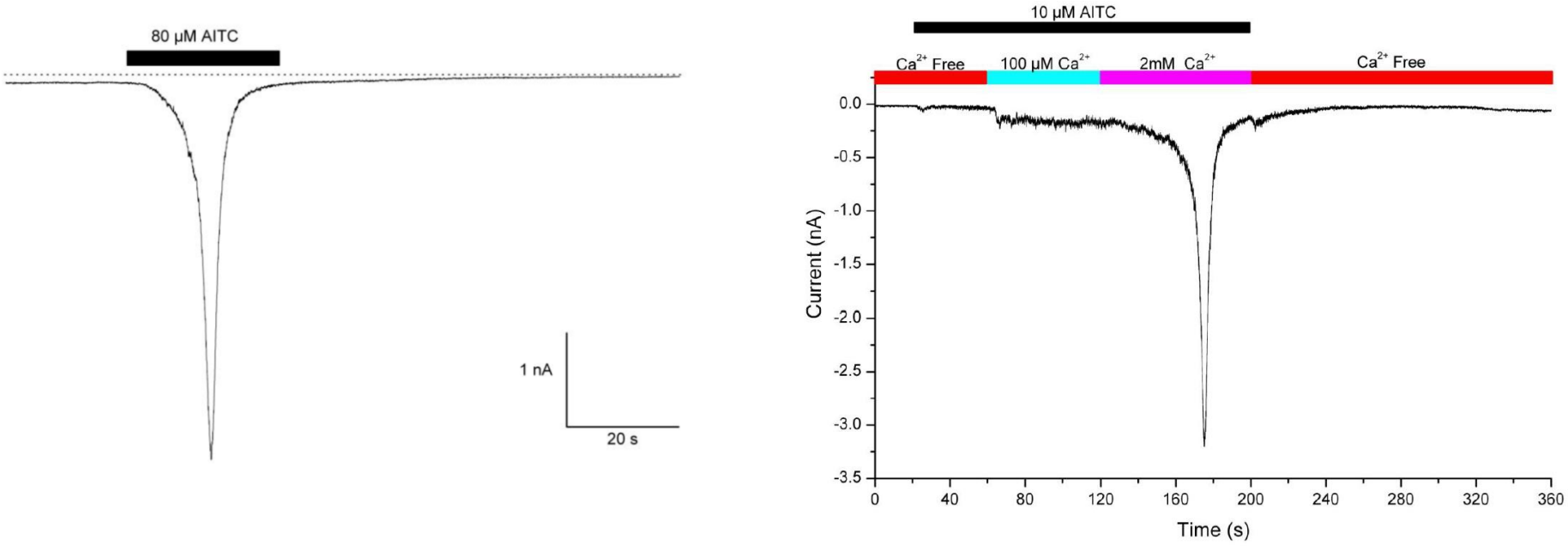

Effect of Ca^{2+} ions on hTRPA1 kinetics: **Left:** A single application of 80 µM AITC lead to an increase in the amplitude of the inward current, recorded at a holding potential of -40 mV. **Right:** A single application of 10 µM AITC was performed using a rapid solution changer to adjust the external calcium ion concentration. Calcium ion concentration was increased from nominally free to 100 µM and 2 mM in the continued presence of 10 µM AITC with a holding potential of -60 mV. (All experiments were performed at room temperature (22-23°C), Manual Patch Clamp Data)

TRPA1

BACK

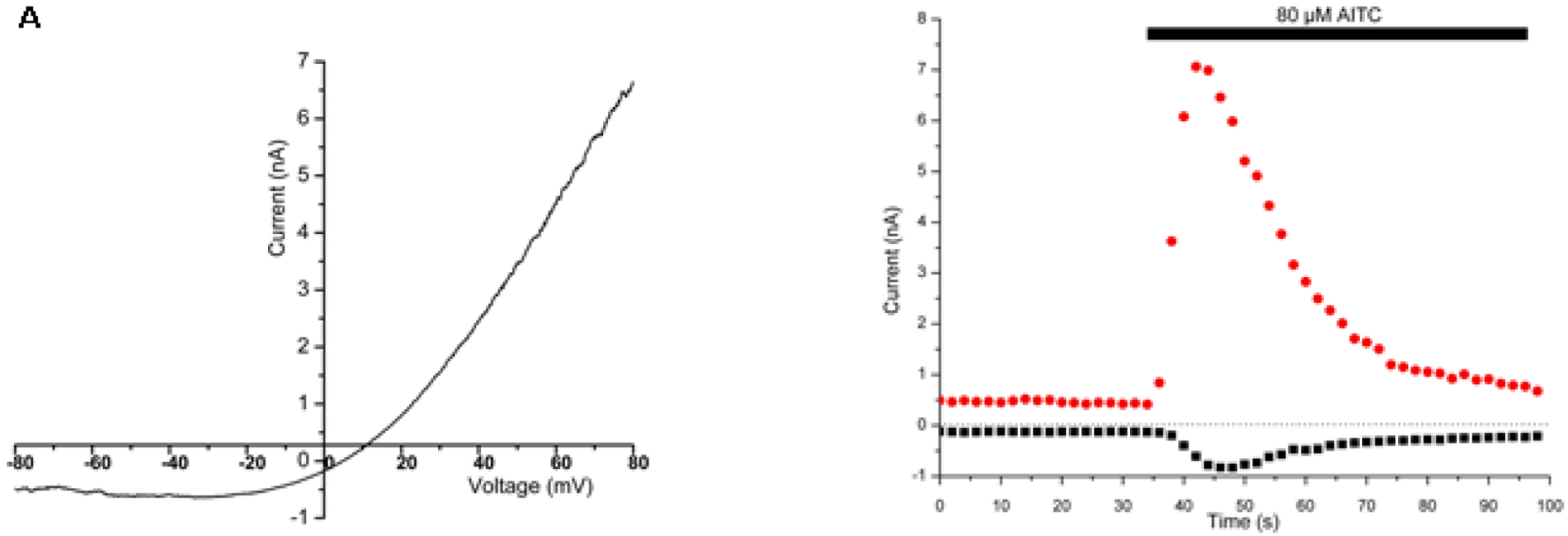

hTRPA1 Current-Voltage (I/V) Ramp Characteristics: **Left:** I/V relationship. Voltage ramps were applied from –80 mV to +80 mV from a holding potential of -70 mV, every 2 seconds. Currents elicited immediately before addition of AITC has been subtracted from the peak AITC current. **Right:** Time-course of AITC-evoked response at +80 mV (red circles) and -80 mV (black squares) (PatchXpress Data).

TRPA1

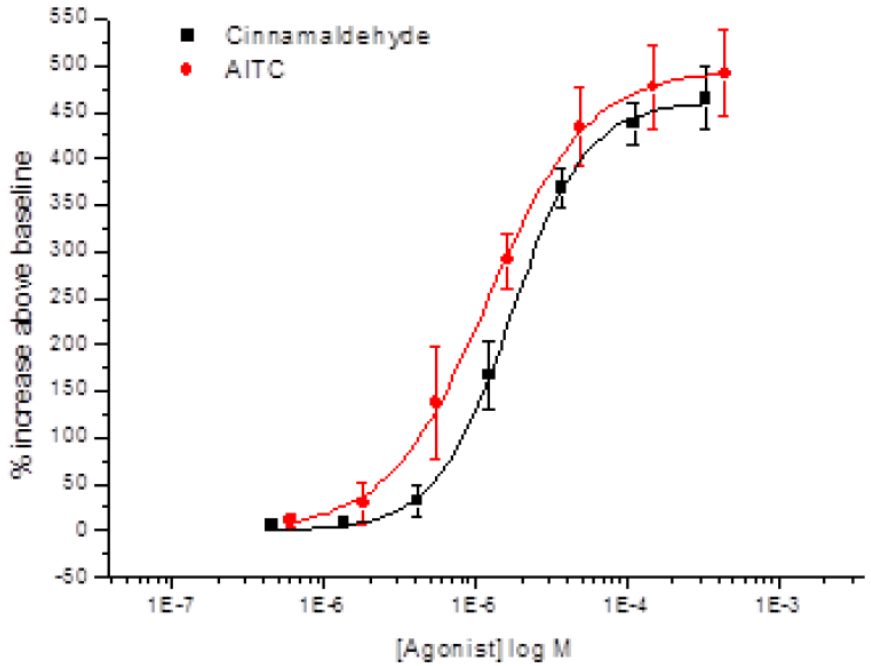

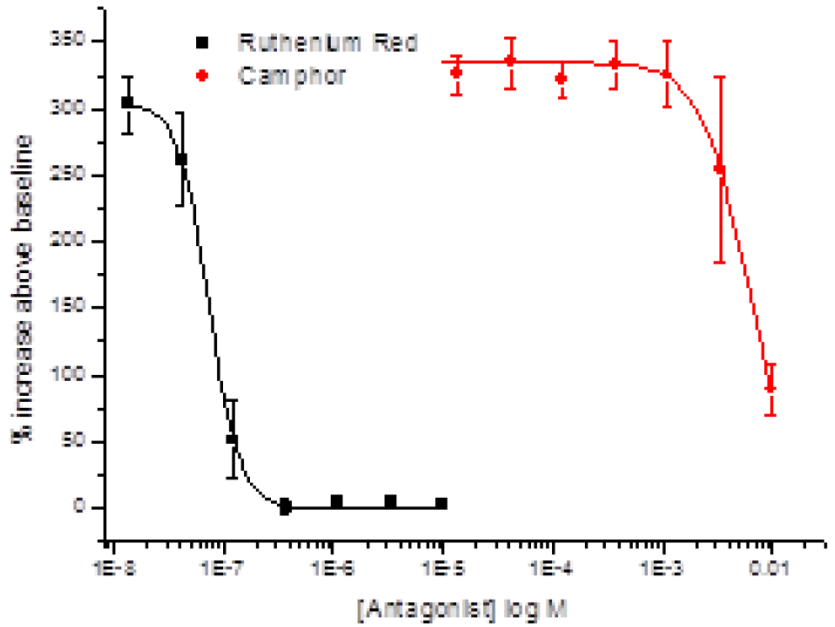

BACK

hTRPA1 Agonist Dose-Responses of Cinnamaldehyde- and AITC-activation, Antagonist Pharmacology: EC_{50} = 12.0 ± 0.5 µM (AITC) and 15.7 ± 1.3 µM (Cinnamaldehyde). Each data point represents mean ± SEM, n=6 (Cinnamaldehyde) or 3 (AITC) independent experiments **Right:** IC_{50} = 73.4 ± 1.9 nM (RR) and approximately 6 mM (Camphor). Each data point represents mean ± SEM, n=4 (ruthenium red) or n=3 (camphor) independent experiments. (FlexStation Calcium Flux Data).

TRPA1

BACK

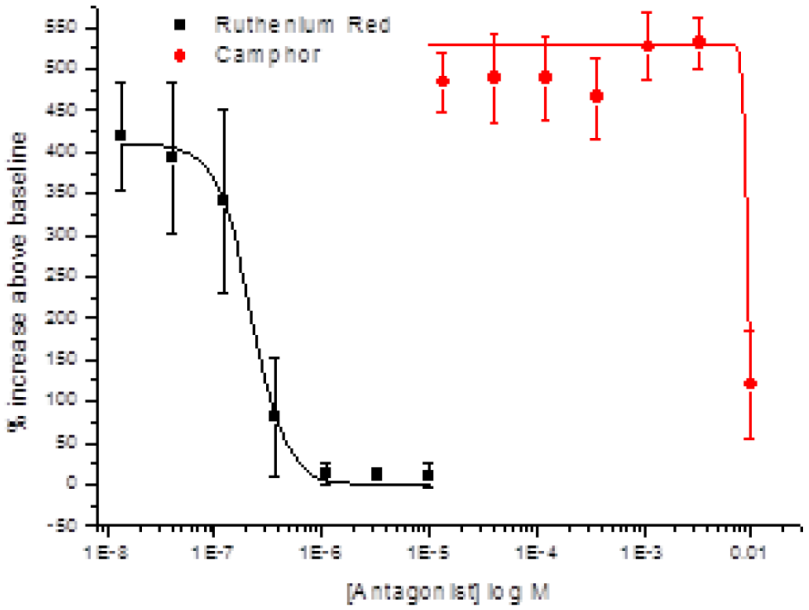

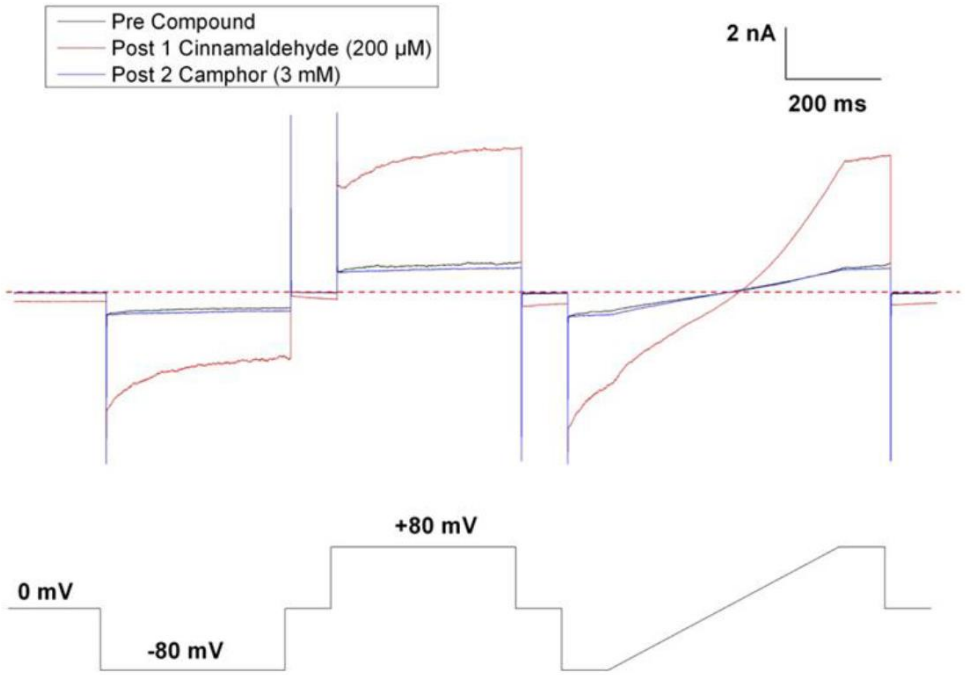

hTRPA1 Antagonist Pharmacology: IC_{50} = 222.0 ± 12.8 nM (RR) and approximately 10 mM (Camphor). Each data point represents mean ± SEM, n=3 independent experiments (FlexStation Calcium Flux Data). **Right:** Currents were evoked using the voltage protocol depicted in the lowest panel before (upper panel) and in the presence of 2-APB (middle panel, 2-APB). The voltage protocol used is shown in the lower panel (voltages in mV) (FlexStation Calcium Flux Data).

BACK

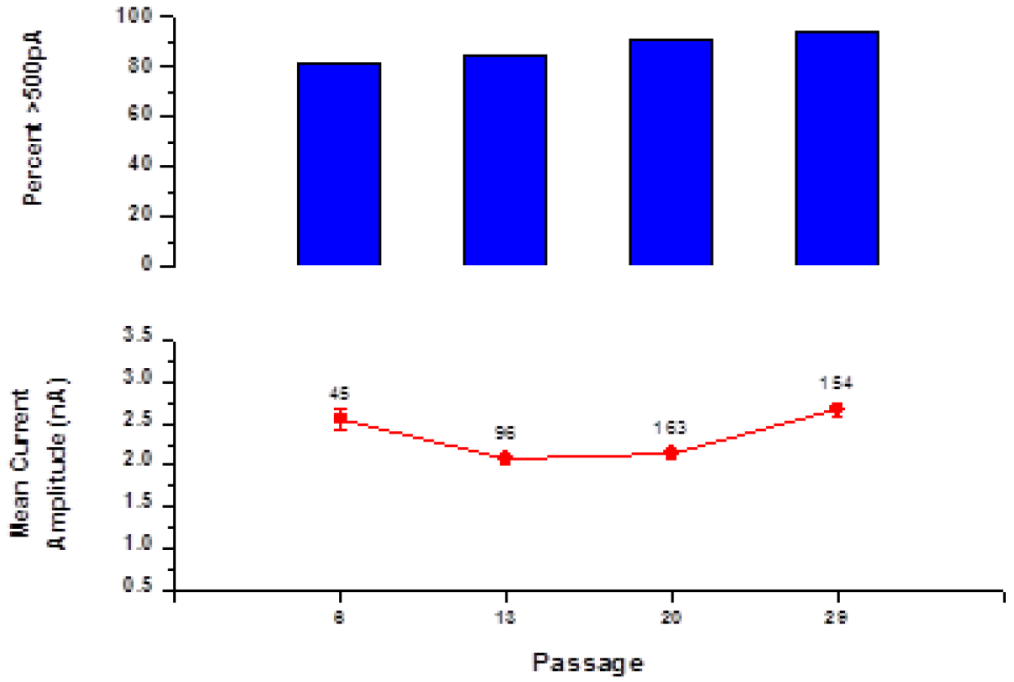

hTRPA1 Stability of Expression over Passage: Upper panel: Percentage of cells expressing a mean peak current >500 pA at +80 mV at cell passages 6, 13, 20 and 29. Lower panel: Mean current amplitude (mean ± SEM, red circles) and the number of cells (numbers above red circles - out of 64 cells for passage 6, 128 cells for passage 13 and out of 192 cells for passages 20 and 29). (IonWorks HT Data).

TRPV1 (CYL3063)

eurofins | DiscoverX
The Eurofins Discovery PRODUCTS COMPANY

BACK

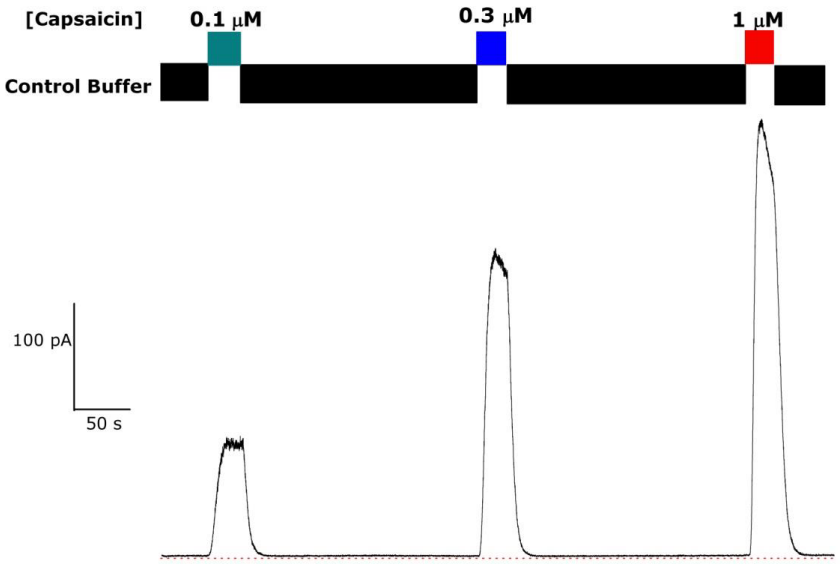

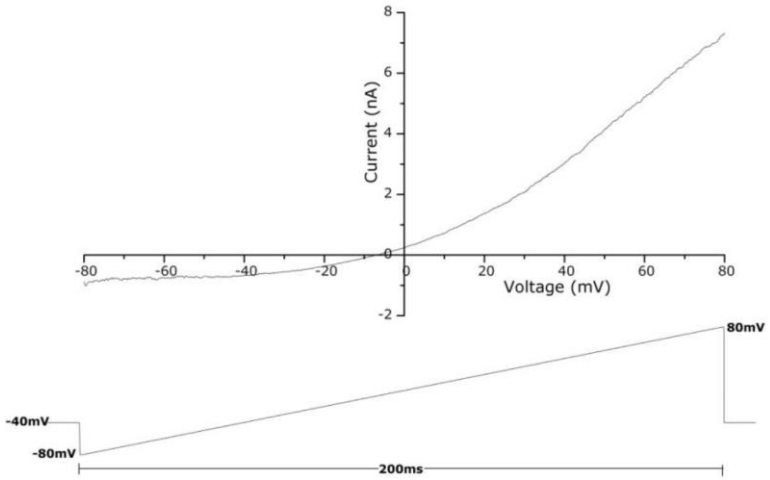

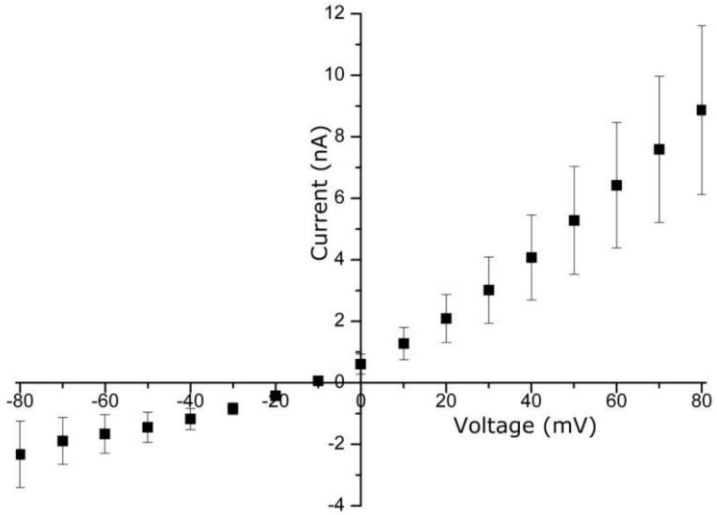

Effect of Capsaicin on hTRPV1 currents and Current-Voltage (I/V) relationship. **Left:** Cells were clamped at a holding potential of +20 mV and perfused with external buffer. Increasing concentrations of capsaicin were briefly pulsed on to the cell and immediately washed off. Zero current level is shown as the red dotted line. **Middle: TRPV1 Current-Voltage (IV) Relationship Evoked by Capsaicin.** Cells were held at a membrane potential of -40 mV and ramped from –80 mV to +80 mV over 200 ms before and during addition of 0.3 µM capsaicin. The leak-subtracted I/V relationship exhibits outward rectification. **Right:** The mean I/V relationship for capsaicin-evoked currents was obtained by measuring the current evoked at various voltages (–80 mV to +80 mV in 10 mV increments) from individual I/V relationships as shown in the Middle Panel (Manual Patch Clamp Data).

BACK

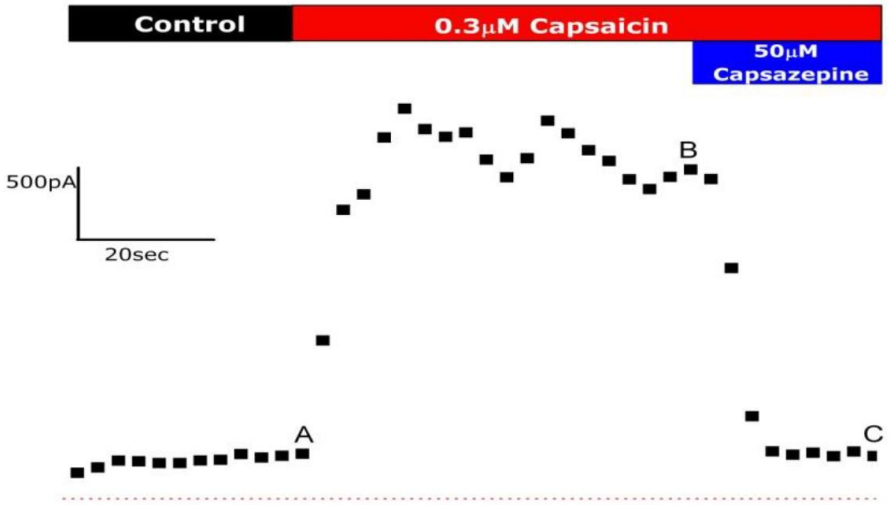

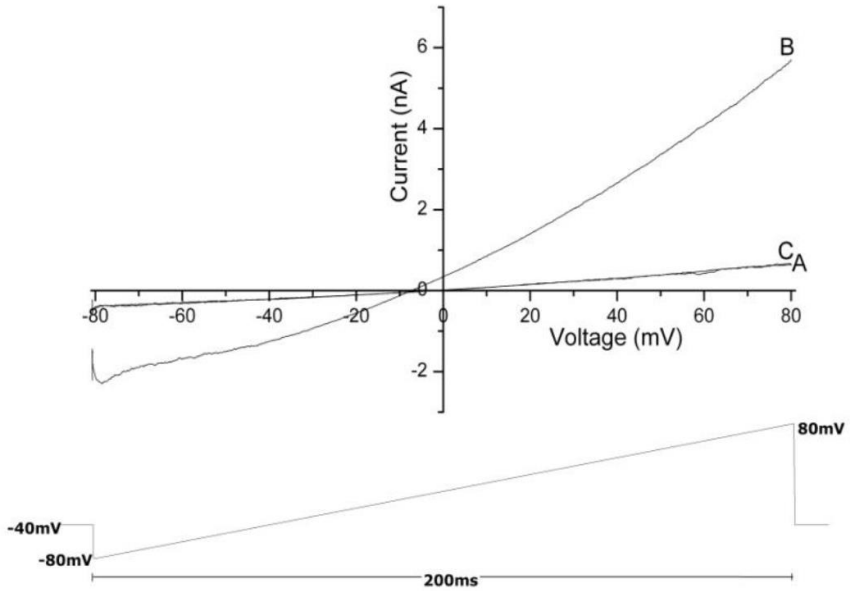

Effect of Capsazepine on hTRPV1 Currents Evoked by Capsaicin: **Left:** Long-term record from a representative cell of currents sampled at +40mV every 3 seconds. **Right:** Current traces taken at points A, B and C from the cell held at a potential of -40 mV and ramped from –80 mV to +80 mV over 200 ms with an interpulse interval of 3 seconds (Manual Patch Clamp Data).

TRPV1

BACK

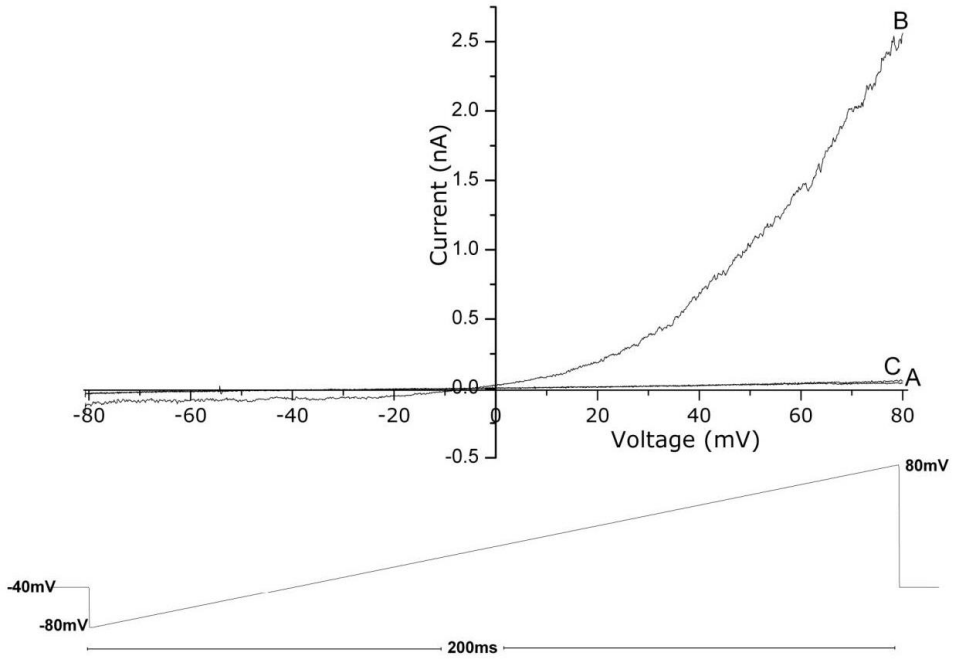

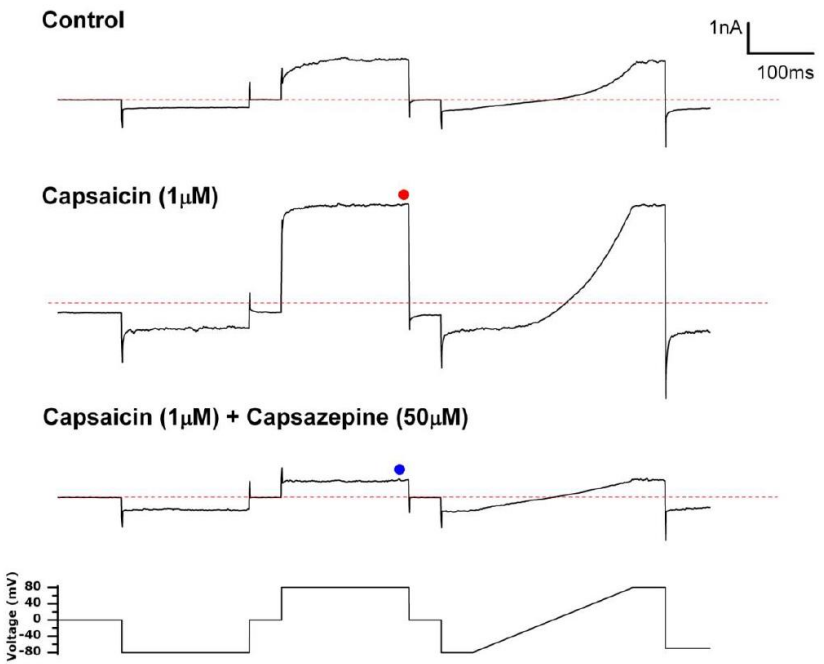

Inhibition of hTRPV1 Current by SB-366791 and Capsazepine: **Left:** A representative cell held at potential of -40 mV and ramped from –80 mV to +80 mV over 200 ms with an interpulse interval of 3 seconds. The cell was held in control buffer (A) and then buffer containing 0.1 μM Capsaicin was perfused over the cell, resulting in increased current (B) that was abolished after addition of 10 nM SB-366791 (C) (Manual Patch Clamp Data). **Right:** Currents were evoked using the voltage protocol depicted in the lowest panel before (1st panel, Control), in the presence of capsaicin (2nd panel, Capsaicin) and in the presence of capsaicin and capsazepine (3rd panel). (IonWorks HT Data).

TRPV1

BACK

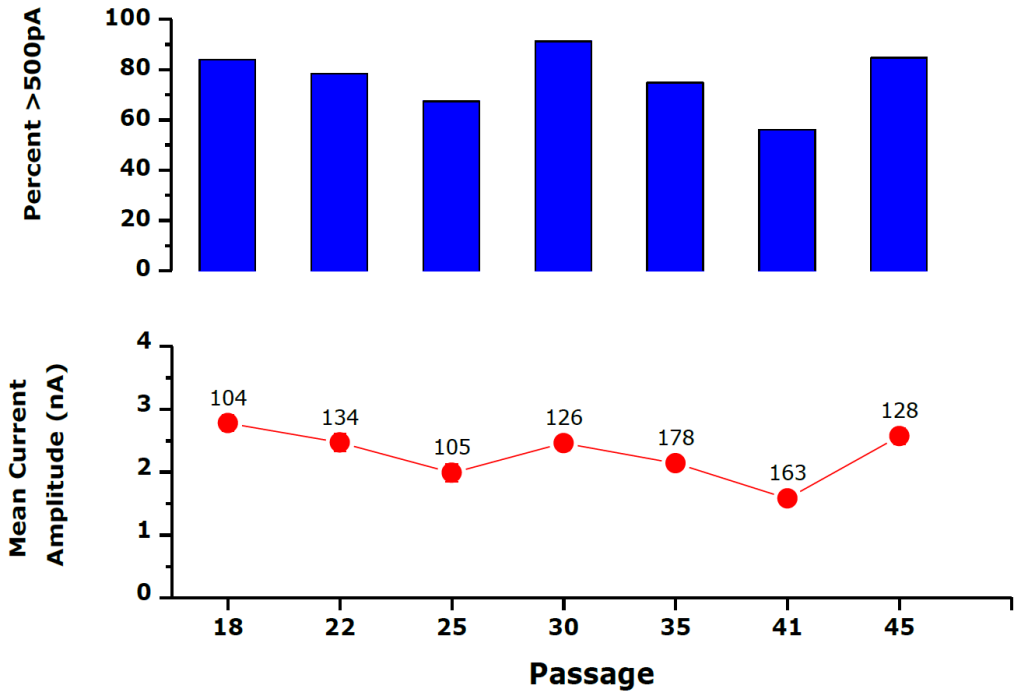

hTRPV1 Stability of Expression Over Passage: **Left:** The upper panel shows the percentage of cells expressing a mean peak current >500 pA at +80 mV at cell passages 18, 22, 25, 28, 30, 35, 41 and 45. The lower panel shows the mean current amplitude (mean ± SEM, red circles) and the number of cells (numbers above red circles - out of 192 cells for all passages) (IonWorks HT Data).

TRPV3 (CYL3065)

BACK

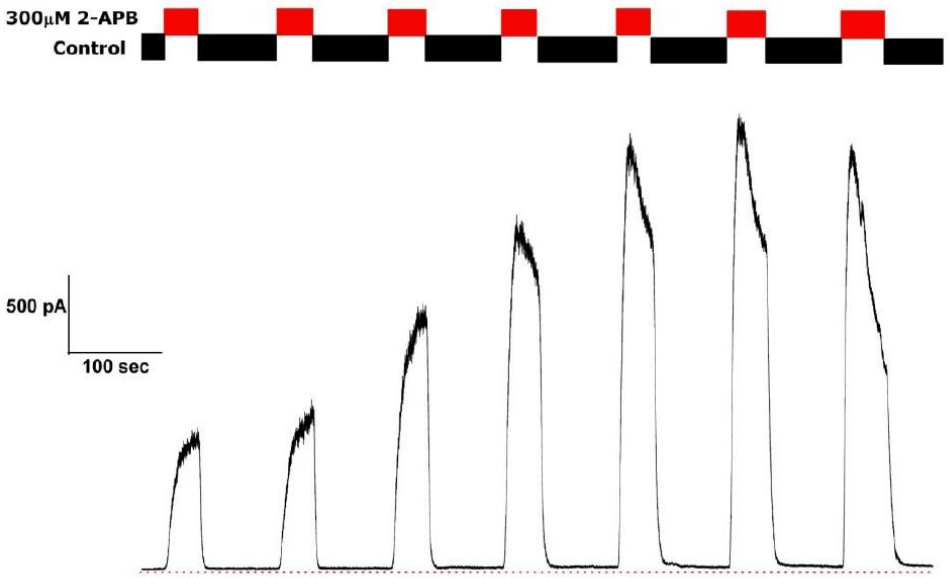

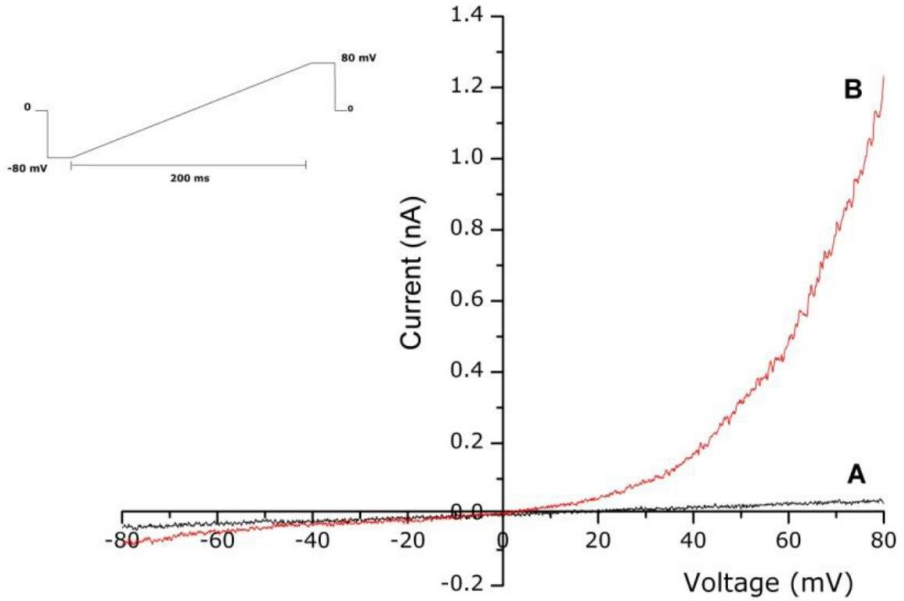

Activation of hTRPV3 by Sequential Applications of 2-APB and Current-Voltage (I/V) Characteristics: **Left:** applications of 2-APB lead to a progressive increase in the amplitude of the outward current, recorded at +40 mV. All experiments were performed at room temperature (22-23°C).**Right:** Voltage ramps (inset) were applied from –80 mV to +80 mV from a holding potential of 0 mV, every 2 seconds. Ramps were applied before (A) and in the presence of 300 µM 2-APB (B). (Manual Patch Clamp Data).

BACK

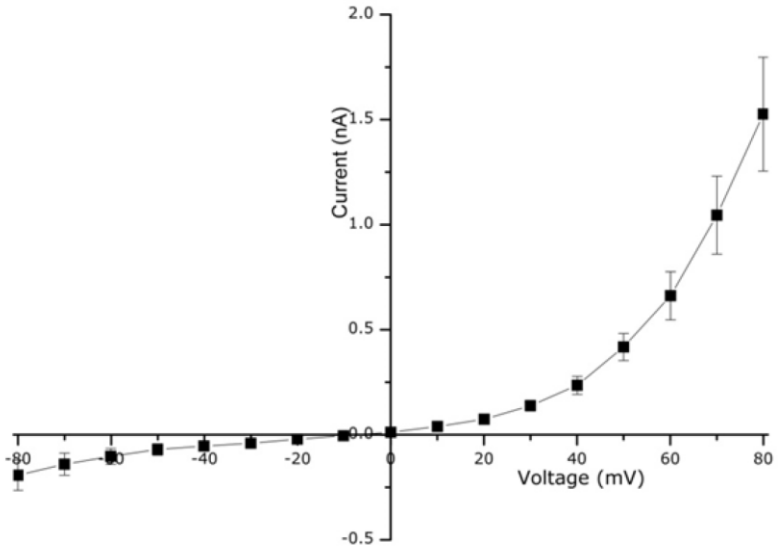

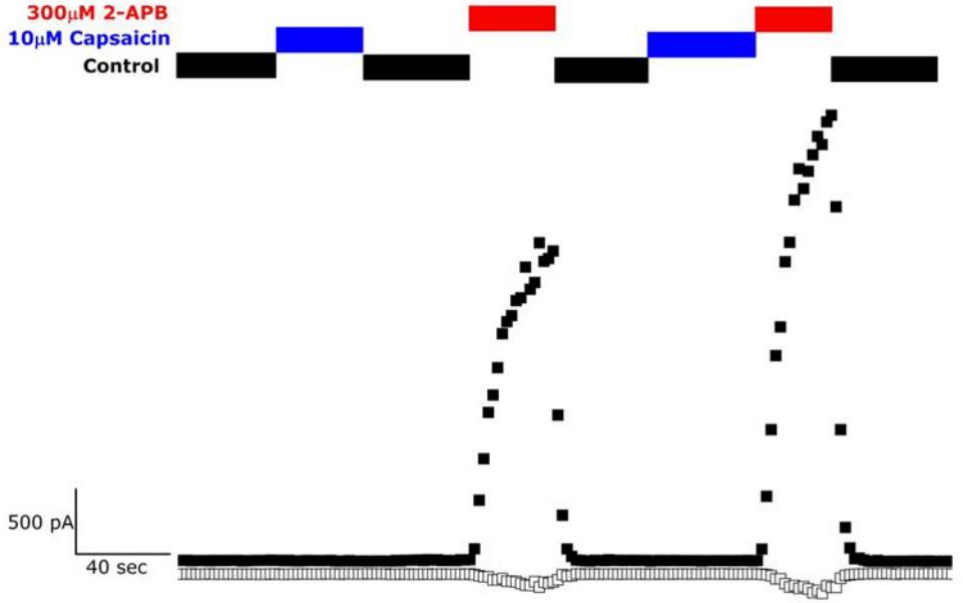

Mean I/V Characteristic of hTRPV3 Currents and hTRPV3 Currents Evoked by 2-APB but not by Capsaicin: **Left:** The data was obtained from the voltage ramp data illustrated in the previous Figure and is the mean of 5 cells in the presence of 300 µM 2-APB **Right:** Capsaicin (blue bars) failed to evoke any current at either +80 mV (solid squares) or –80 mV (open squares). Addition of 2-APB (red bars) evoked significant outward currents at +80 mV and a detectible current at –80 mV (Manual Patch Clamp Data).

TRPV3

BACK

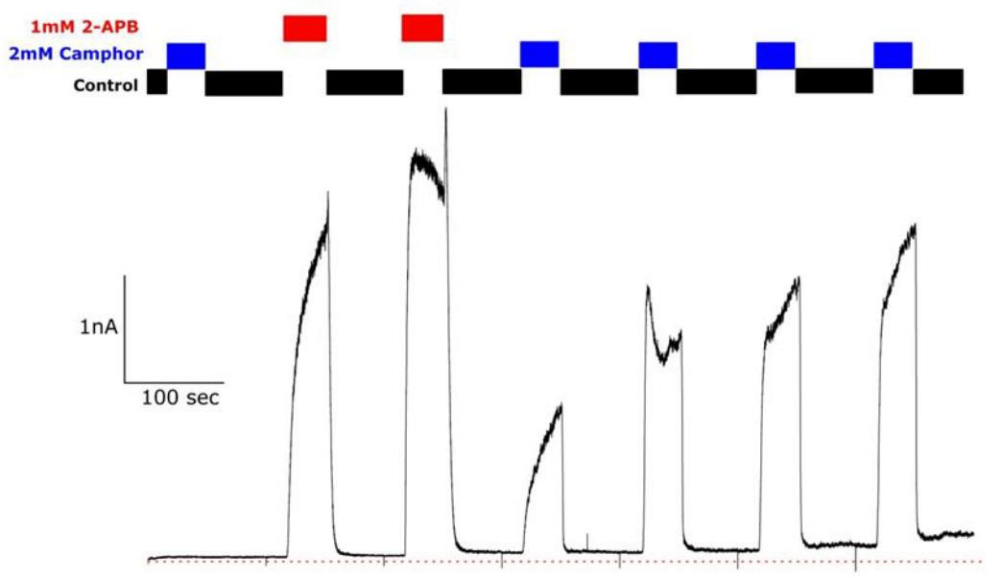

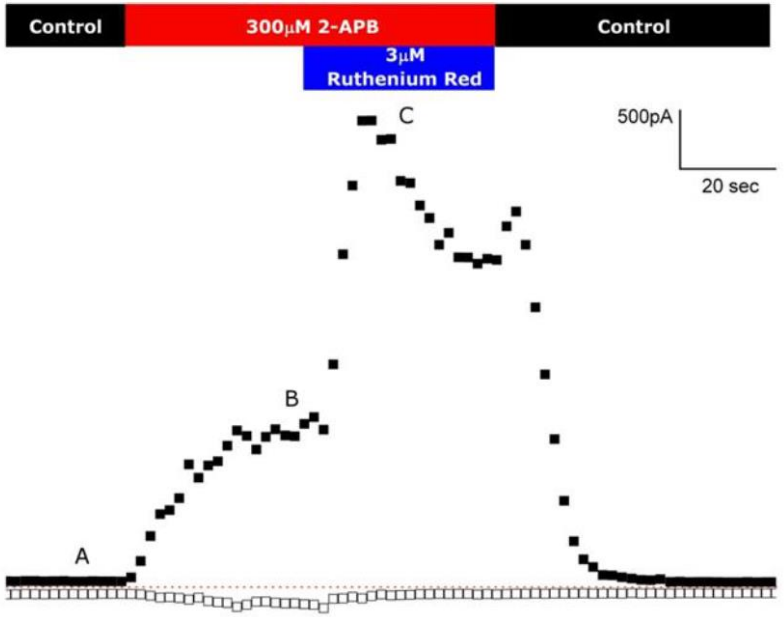

Low Doses of Camphor Only Activate hTRPV3 After Sensitization with 2-APB and Effect of Ruthenium Red: **Left:** The first addition of camphor (blue bars) failed to evoke any outward current from a holding potential of +40 mV. Subsequent additions, after 1 mM 2-APB (red bars) evoked outward currents of successively increasing amplitude. **Right:** 2-APB (300 µM) evoked a significant outward current at +80 mV (solid squares) that reached a steady amplitude at (B). There was a corresponding small increase in inward current at –80 mV (open squares). Addition of ruthenium red (blue bar) markedly increased the current amplitude at +80 mV reaching a peak at (C). The corresponding inward current at –80 mV was completely blocked. (Manual Patch Clamp Data).

BACK

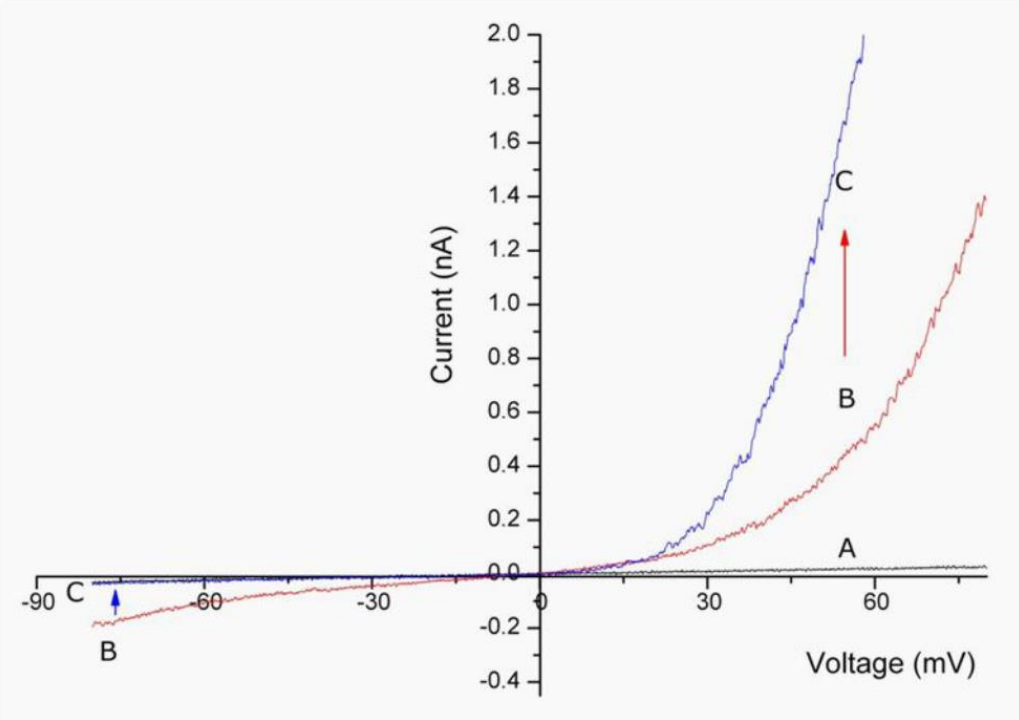

Effect of ruthenium red on hTRPV3: Prior to any additions, 200 ms ramps from –80 mV to +80 mV evoked a small linear leak current (A, black trace). Addition of 2-APB (300 µM) evoked an outwardly rectifying current that produced some inward current at negative voltages (B, red trace). Addition of ruthenium red markedly potentiated the current at positive potentials (C, blue trace, red arrow) but completely abolished the current at negative potentials (blue arrow). (Manual Patch Clamp Data).

TRPV3

BACK

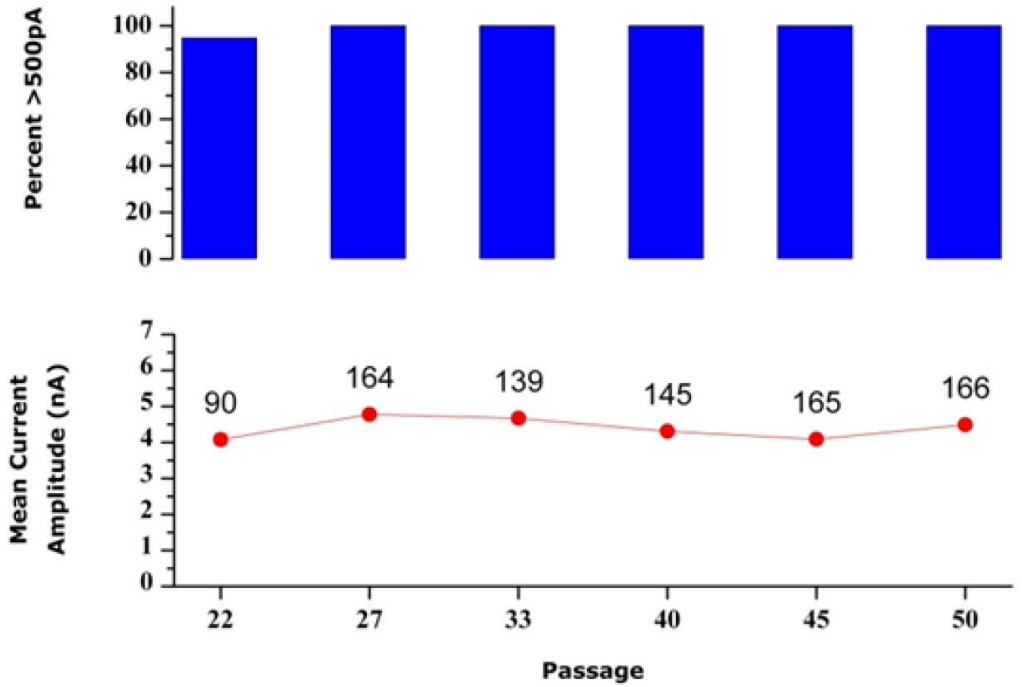

Monitoring hTRPV3 Expression using IonWorks Stability of Expression over Passage: **Left:** Currents were evoked using the voltage protocol depicted in the lowest panel before (upper panel) and in the presence of 2-APB (middle panel, 2-APB). The voltage protocol used is shown in the lower panel (voltages in mV). **Right:** The upper panel shows the percentage of cells expressing a mean peak current >500 pA at +100 mV at cell passages 22, 27, 33, 40, 45 and 50. The lower panel shows the mean current amplitude (mean ± SEM, red circles) and the number of cells (numbers above red circles - out of 192 cells for all passages). (IonWorks HT Data).

TRPV4 (CYL3064)

BACK

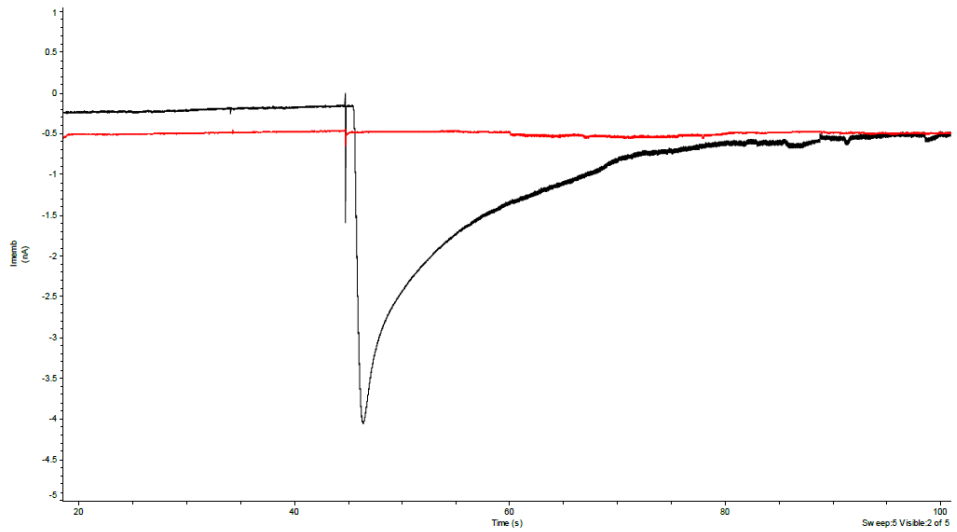

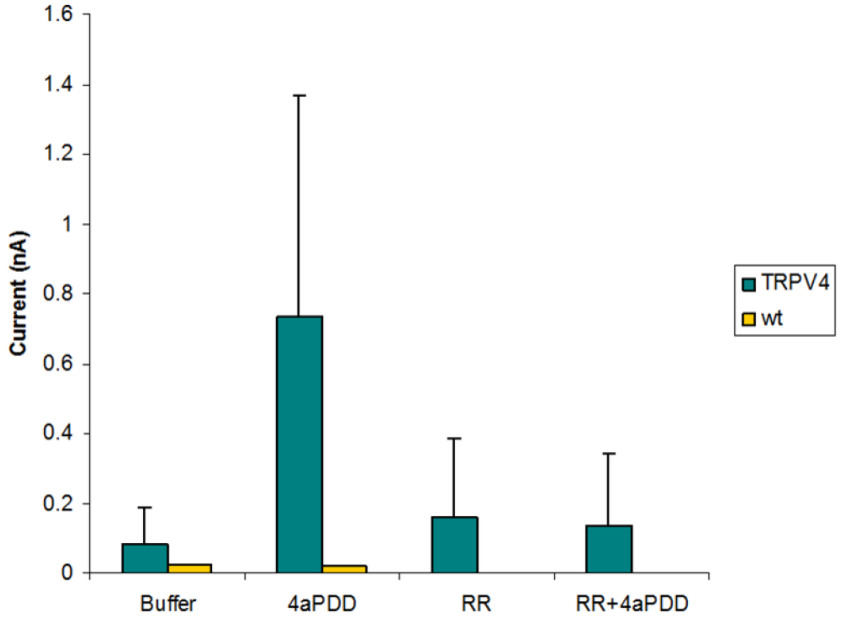

hTRPV4 Agonist and Antagonist Characterization and Activation by 4αPDD: **Left:** TRPV4 currents are activated with 10 µM GSK1016790A and blocked with 10 µM ruthenium red. hTRPV4 currents were recorded in physiological saline (137 mM NaCl, 4 mM KCl, 1 mM MgCl2, 1.8 mM CaCl2, 10 mM HEPES and 10 mM Glucose, pH 7.3) from cells held at -60 mV. The current shown in black was obtained in response to addition of 10 µM GSK1016790A, and the red trace is the response to the GSK compound after a three-minute preincubation with 10 µM ruthenium red .**Right:** 10 µM 4αPDD elicited large inward currents in hTRPV4-HEK, cells, but not in untransfected host wild-type (wt) cells. The current in response to 10 µM 4αPDD was blocked by a three-minute preincubation with 10 µM ruthenium red. The bars represent the average and SD of N = 4 cells. (PatchXpress Data).

BACK

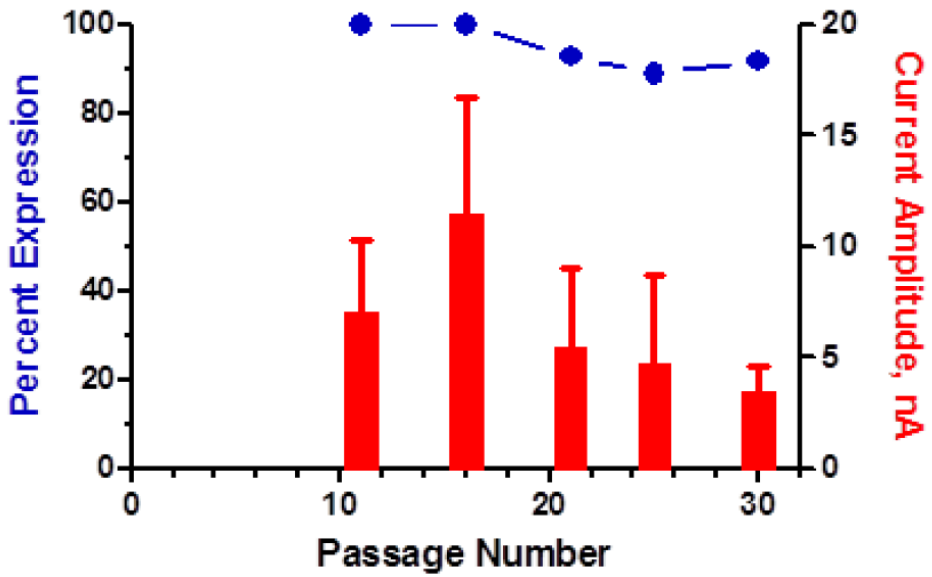

hTRPV4 Stability of Expression over Passage: Stability of expression and current amplitude. The blue line shows the percentage of cells expressing a mean peak inward current >0.25 nA at –60 mV in response to addition of 10 µM GSK1016790A at cell passages 11, 16, 21, and 25. The red bars show the mean current amplitude (mean ± SD) for 5-13 cells per experiment (PatchXpress Data).

TRPV4

BACK

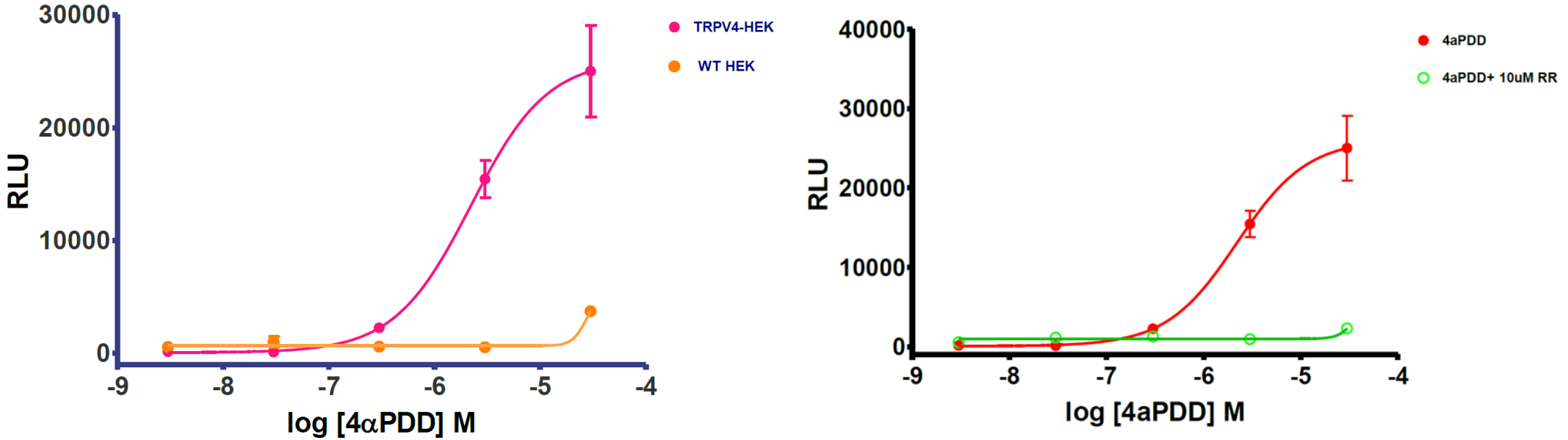

hTRPV4 Pharmacological Characterizaion in a Calcium Flux Assay: **Left:** TRPV4-HEK cells, but not the WT-HEK cells responded to 4αPDD in a concentration-dependent manner. Each data point is the mean and SD of four wells. The EC_{50} value for the TRPV4 cell line was 2.2 µM, and the Hill slope was 1.2. **Right:** Preincubation with 10 µM ruthenium red blocked 4αPDD-induced calcium flux. Each data point is the mean and SD of four wells. (FLIPR Calcium Flux Data).

TRPV4

BACK

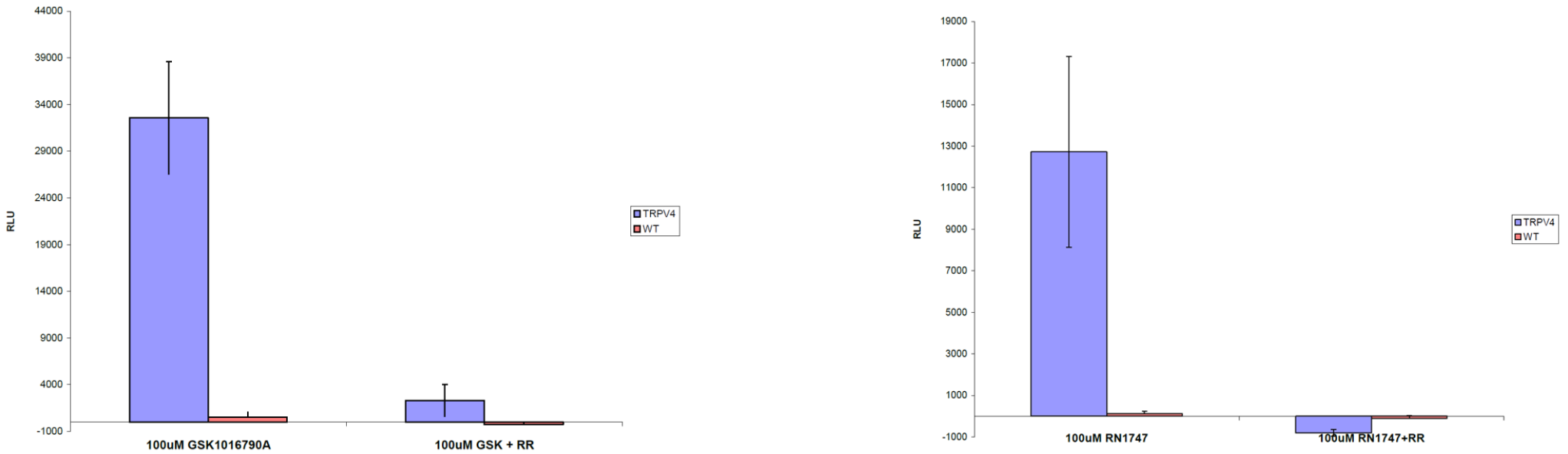

hTRPV4 Pharmacological Characterizaion in a Calcium Flux Assay: **Left:** hTRPV4-HEK cell stimulation of calcium flux by 100 µM GSK1016790A was blocked by 10µM ruthenium red. The wild-type HEK cells were not activated. Each data point is the mean and SD of four wells. **Right:** hTRPV4-HEK cells were stimulated by 100 µM RN1747. The activation was blocked by 10µM ruthenium red. The wild-type HEK cells were not activated. Each data point is the mean and SD of four wells. (FLIPR Calcium Flux Data).

CFTR (CYL3088)

BACK

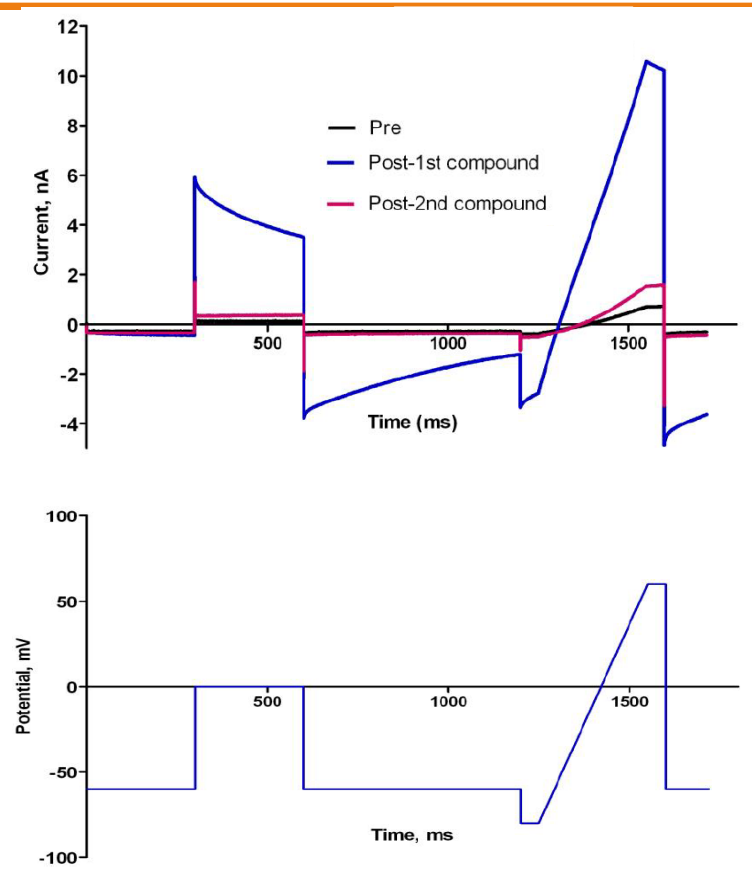

Activation and Inhibition of hCFTR Current. hCFTR currents (top) evoked by a two-part voltage protocol: The voltage ramp shown was from -80 to +60 mV at a rate of 0.46 mV/s. The CFTR current was defined as the peak total current between 302 and 345 msec present at 0 mV during the first step after a 4-min preincubation with 500 µM 8-bromoadenosine cAMP and 10 µM Genistein (labeled Post 1) minus the current remaining after addition of 10 µM CFTRinh-172 (post 2). The voltage protocol is shown below the current traces. (IonWorks HT Data).

CFTR

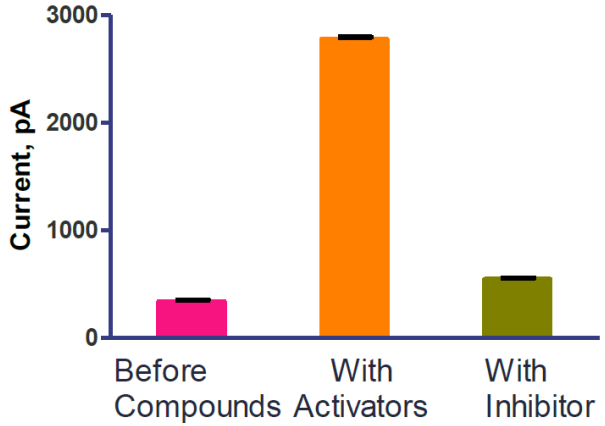

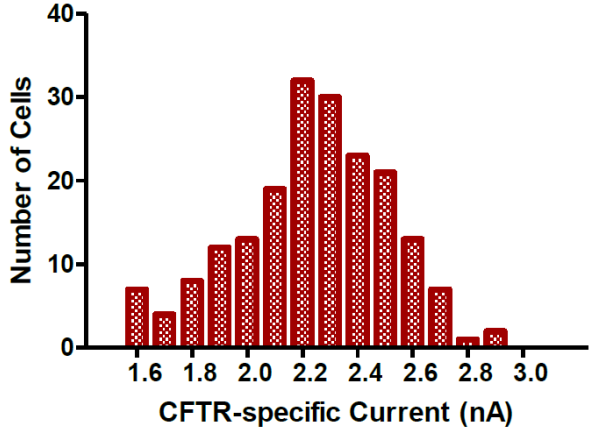

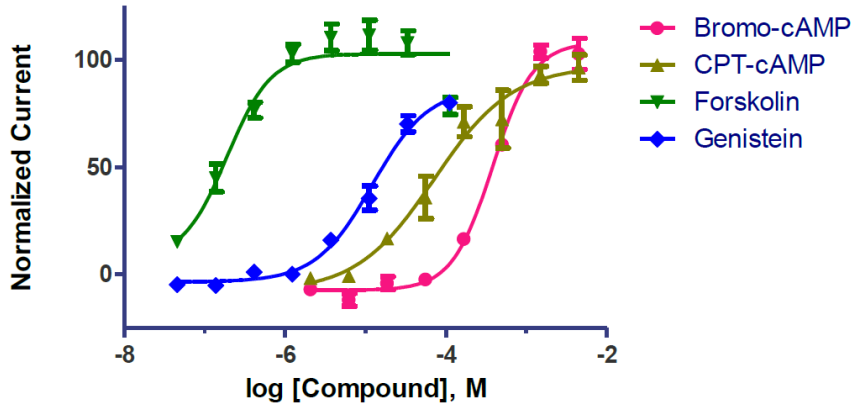

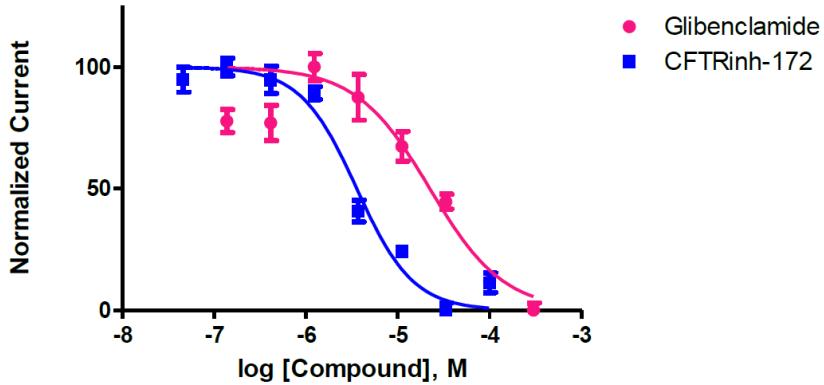

BACK

Activation and inhibition of hCFTR Current: **Left:** A comparison of currents at 0 mV (top) recorded before any compound addition, after addition of the activators 500 µM 8-bromoadenosine cAMP and 10 µM Genistein, and after addition of specific inhibitor (10 µM CFTRinh-172). N = 191 cells per condition; mean ± SEM. Frequency distribution of current amplitudes (bottom). **Right (Top):** In order to assess hCFTR activators, concentration-response curves were plotted using the activators shown. The EC_{50} values obtained, in rank order of potency, were: Forskolin 0.72 µM, Genistein 12.2 µM, CPT-cAMP 71.9 µM, and Bromo-cAMP 383.2 µM. **Right (Bottom):** CFTR currents were inhibited by Glibenclamide and the CFTR-specific inhibitor CFTRinh-172. The IC_{50} values obtained were 22.4 µM for Glibenclamide and 3.6 µM for CFTRinh-172 (IonWorks HT Data).

ASIC3 (CYL3055)

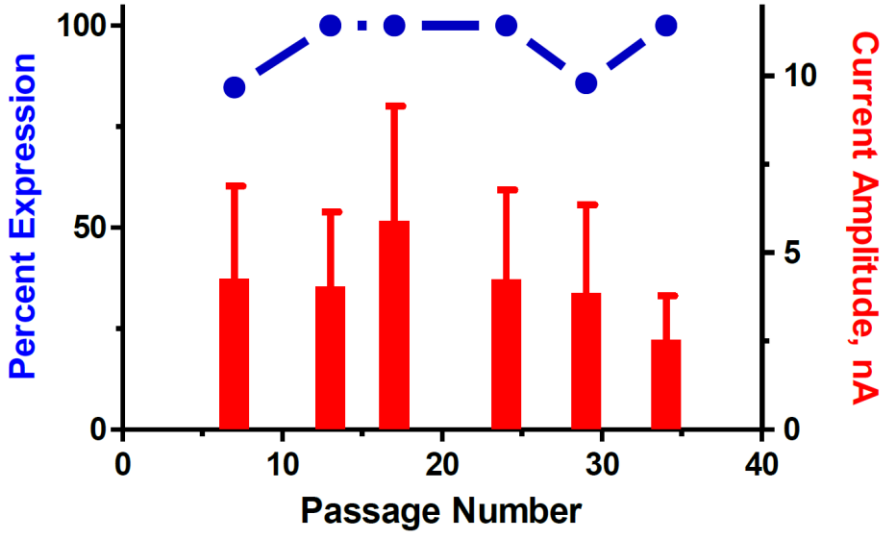

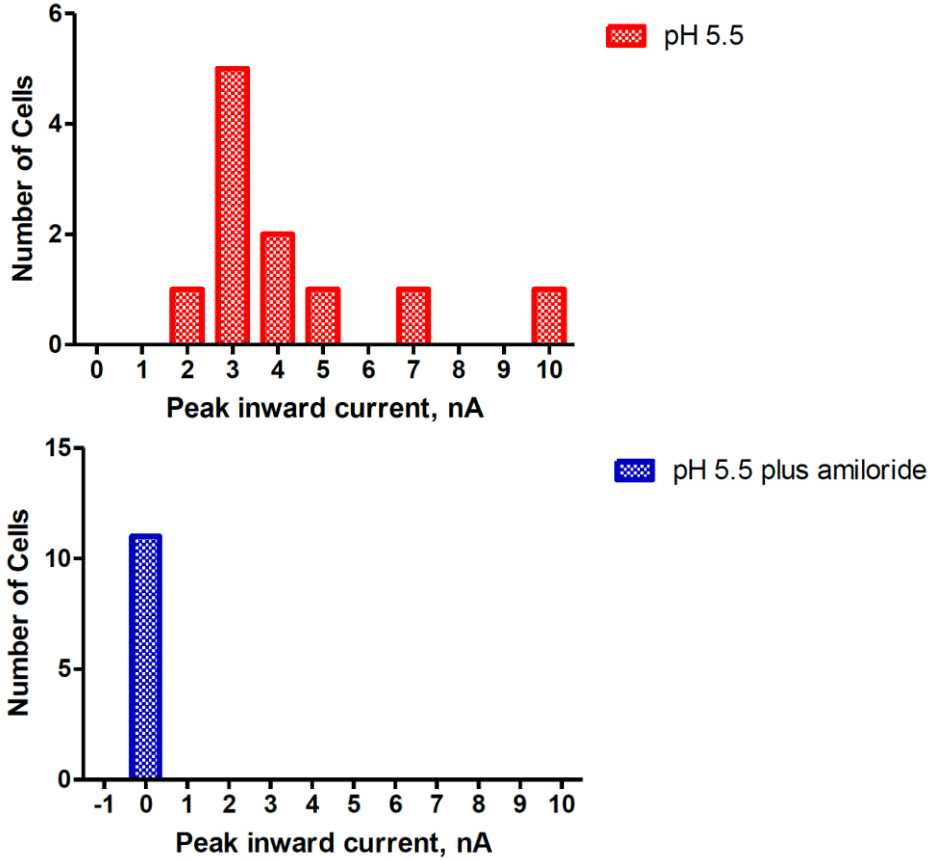

BACK

Stability and Current Amplitudes of hASIC3 Currents: **Left:** Stability of expression and current amplitude. The blue line shows the percentage of cells expressing a mean peak inward current >0.5 nA at –70 mV at cell passages 7, 13, 17, 24, 29 and 34. The red bars show the mean current amplitude (mean ± SD) for 5-15 cells per experiment. At passage 7, 100% of the cells sealed, and 11 out of 13 (84.6%) had currents >0.5 nA following addition of pH 5.5 extracellular solution. **Right (Top):** Typical frequency distributions of current amplitude. Mean current response to addition of pH 5.5 extracellular solution: -4.24 ± 2.28 nA (SD, 11 cells). **Right (Bottom):** After addition of pH 5.5 extracellular solution in the presence of 1 mM amiloride, mean current: -0.05 ± 0.06 nA (SD, 11 cells) (PatchXpress Data).

ASIC3

BACK

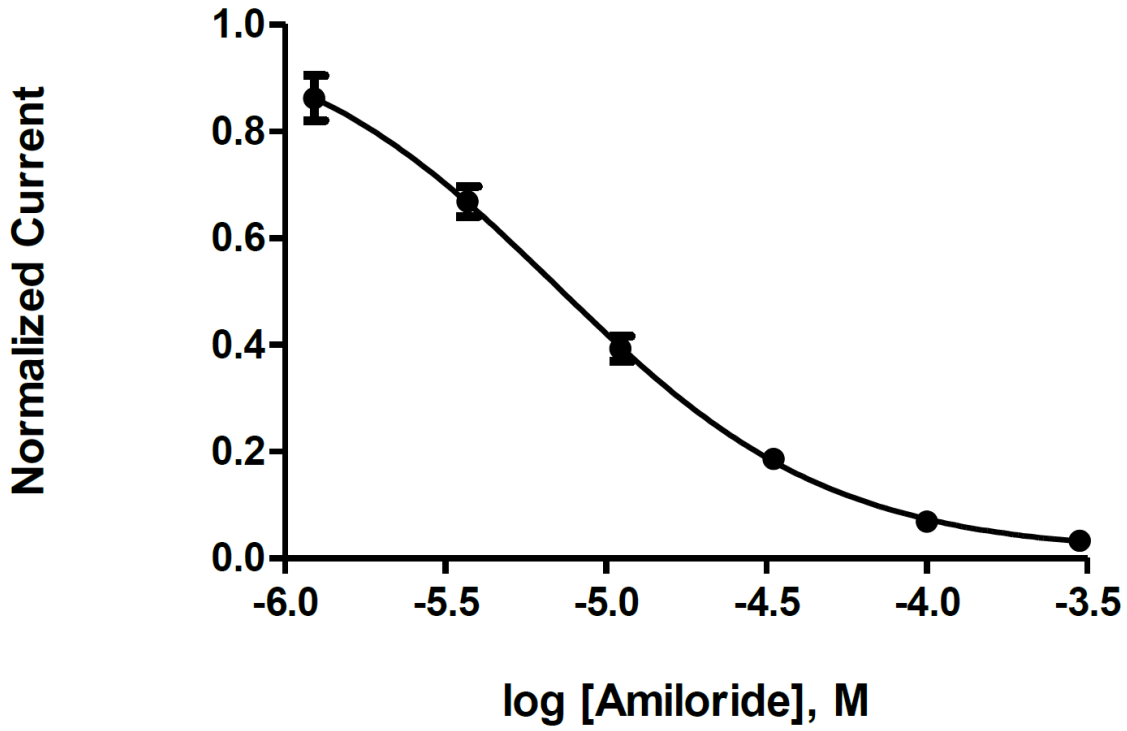

hASIC3 Current Blockade by Amiloride: Inhibition of the current response to addition of pH 5.5 extracellular solution by amiloride. Each point indicates the mean (±SEM) response of 6 cells. We obtained an IC_{50} of 7.0 M and a Hill slope of -1.0. Sutherland et al. obtained an IC_{50} of 63 M for rat ASIC3 expressed in COS-7 cells (PatchXpress Data)